Spectrally narrowed lasing of a self-injection KrF excimer laser

Yasuhiro Shimada, Koichi Wani, Tadaaki Miki, Hidehito Kawahara, Mutsumi Mimasu and Yoshiro Ogata

Electronics Research Laboratory, Matsushita Electronics Corporation
1-1 Saiwai-cho, Takatsuki, Osaka 569, Japan

ABSTRACT

Spectrally narrowed lasing of a KrF excimer laser has been achieved by a self-injection technique using a beam splitter for power extraction and intracavity etalons for spectral-narrowing. The laser cavity is divided into an amplifying branch and a spectral-narrowing branch. The spectral bandwidth was narrowed to < 3 pm FWHM with air-spaced etalons placed in the spectral-narrowing branch. A laser propagation model was introduced for describing the laser intensity traveling in the laser cavity. The calculated intensity incident on the intracavity etalons was smaller than that in the conventional Fabry-Perot cavity with plane-parallel mirrors.

1. INTRODUCTION

Industrial KrF excimer lasers with narrow bandwidth used in optical microlithography require long term stability and extended lifetime. Current techniques for spectral-narrowing are making use of intracavity dispersive or interferometric optics such as gratings, prisms, and etalons together with Fabry-Perot cavities.[1] For high power industrial excimer lasers, these intracavity optics suffer from intense laser power as high as the saturation intensity (>1 MW/cm^2) which causes optical damage resulting in spectral broadening. In addition, at high repetition rate operation of the lasers, thermal drift in laser wavelength selected by these intracavity optics becomes considerable.[2]

We have developed a self-injection KrF excimer laser that can reduce the laser power incident on the intracavity spectral-narrowing elements. In the present paper, we describe an analytical model of the laser intensity propagating in the laser cavity and give a comparison between the analytical and the experimental results. The analytical data are used for calculating the laser intensity incident on the intracavity etalons. Time history of the narrow bandwidth in long term operation of the laser will be discussed.

2. CAVITY CONFIGURATIONS

Figures 1(a) and 1(b) compare the configurations of the conventional and self-injection KrF lasers with narrow bandwidth.

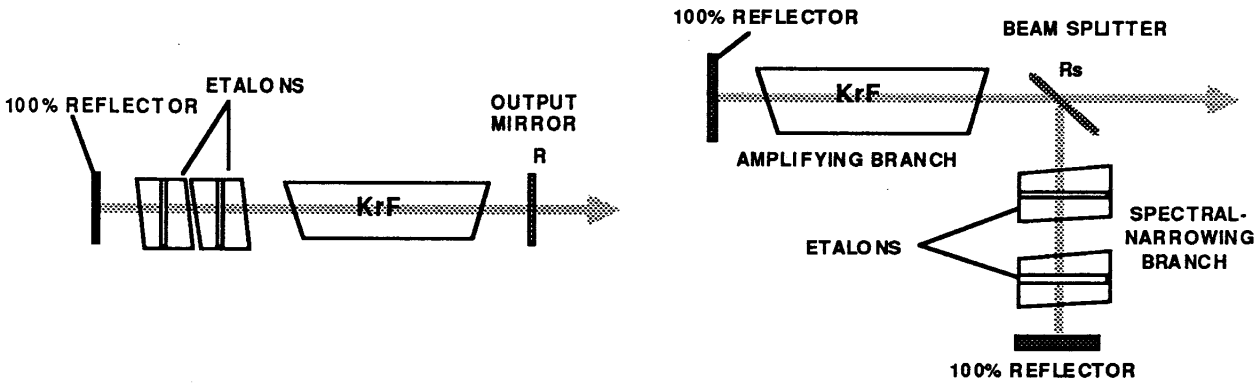

(a) Conventional laser with the Fabry-Perot cavity. (b) The self-injection laser with a beam splitter.

Fig.1 Optical arrangements of spectrally narrowed KrF excimer lasers with intracavity etalons: (a) with a conventional Fabry-Perot cavity, (b) with a beam splitter for power extraction.

Figure 1(a) is the conventional laser with the Fabry-Perot cavity in which a set of two air-spaced etalons for coarse and fine tuning is inserted. Figure 1(b) is the configuration of the laser developed by the authors. The laser cavity has two totally reflecting mirrors constructing the resonator and a partially reflecting mirror used as beam splitter, and is divided into an amplifying branch and a spectral-narrowing branch by the beam splitter. The etalons are placed in the spectral-narrowing branch which produce a seed beam with narrow bandwidth to be injected back into the amplifying branch. The amplified laser beam with narrow bandwidth is extracted through the beam splitter in the direction of the optical axis of the amplifying branch. The laser intensity incident on the intracavity etalons is adjustable by changing the reflectivity of the beam splitter.

Free spectral ranges of the coarse and fine etalons are 430 pm and 43 pm, respectively. The effective finesses for both etalons are better than 10 giving narrow band oscillation with < 3 pm FWHM. A UV-preionized discharge chamber with a 2x1x45 cm^3 active volume[3] was used in both arrangements of the lasers. The discharge chamber was filled with a mixture of 5% Kr and 0.25 % F_2 in He at 1400 Torr.

3. ANALYSIS OF CAVITY PERFORMANCE

The effective lifetime of KrF* (B state) under gas pressure over 1 atm is estimated to be shorter than the radiative lifetime (≈ 6.5 ns)[4] due to collisional quenching. On the other hand, since the observed laser pulse duration of the lasers with narrow bandwidth was 18 ns FWHM and it is much longer than the effective lifetime of the KrF*, the performance of the lasers can be analyzed with a steady-state approximation. The analysis was carried out using a modified version of the laser propagation model given by Rigrod.[5]

A schematic representation of the laser propagation model for the laser with a conventional Fabry-Perot cavity is shown in Fig.2. Both sides of the active region are unpumped, which absorb a fraction a of the laser power incident on them. For simplicity, the absorption losses in the medium of the oscillator windows, mirrors, and environmental atmosphere are included in the factor a. Taking the z axis along with the direction of laser propagation, the laser intensity I is the sum of two counterpropagating components I_+ and I_- at any position z in the cavity. These intensities then increase with propagating distance in the active region according to the differential equations

$$\pm \frac{1}{I_\pm}\frac{dI_\pm}{dz} = \frac{g_0}{1+(I_+ + I_-)/I_s} \quad , \tag{1}$$

where g_0 is the small-signal gain coefficient and I_s is the saturation intensity. Here the constant distributed loss in the active region is neglected. These equations can be integrated over the length of the active region defined by the following boundary conditions:

$$I_+(0) = I_-(0)R_a \qquad \text{and} \qquad I_-(L) = I_+(L)R_b \quad , \tag{2}$$

where the parameters R_a and R_b are the effective reflectivities[6] of the left and right hand sides of the cavity, and L is the length of the active region. Combining all these relations, we obtain the following solutions in the steady-state:

$$\frac{I_-(0)}{I_s} = \frac{r_b}{(r_a + r_b)(1 - r_a r_b)}\left[g_0 L + \ln(r_a r_b)\right]$$

and (3)

$$\frac{I_+(L)}{I_s} = \frac{r_a}{(r_a + r_b)(1 - r_a r_b)}\left[g_0 L + \ln(r_a r_b)\right] \quad ,$$

where $r_a = R_a^{1/2}$ and $r_b = R_b^{1/2}$. The effective reflectivities R_a and R_b are determined by considering the configuration of the laser optics. When the parameters g_0 and I_s are known, the laser intensity propagating in the cavity can be calculated from the above equations.

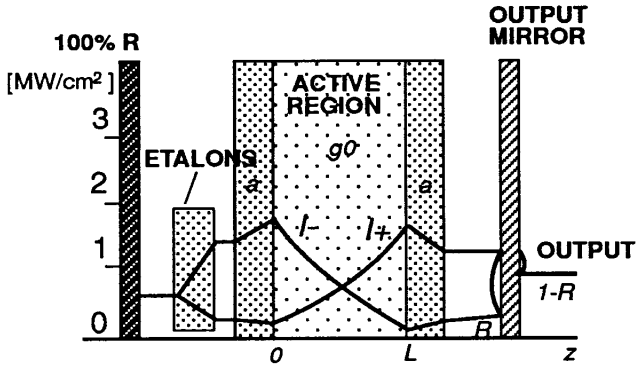

Fig.2 Schematic representation of the laser propagation model for the laser with a conventional cavity.

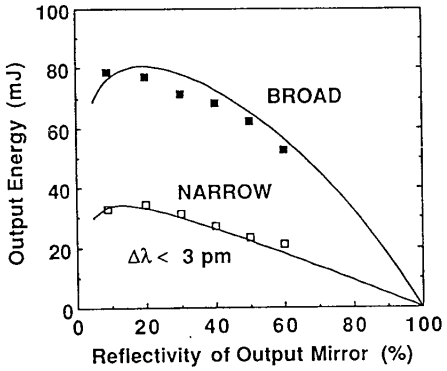

Fig.3 Dependence of the output energy on reflectivity of the output mirror for the laser with the conventional cavity. The traces are calculated from eqs.(3), (4), and (5). Upper trace: broad band laser output without intracavity etalons. Lower trace: narrow band laser output with intracavity etalons.

In order to determine the parameters g_0 and I_s, we calculated the output energy from eqs.(3) to fit the experimental data for the laser with the conventional cavity as a function of the reflectivity of the output mirror. The observed output energy of the laser with the conventional Fabry-Perot cavity is shown in Fig.3. In the broad band oscillation without intracavity etalons, the effective reflectivities of this cavity used in the calculation are given by

$$R_a = (1 - a)^2 \qquad \text{and} \qquad R_b = (1 - a)^2 R \quad , \tag{4}$$

where R is the reflectivity of the output mirror. The fittings of the data gave g_0 = 8.5%/cm, I_s = 1.4 MW/cm², and a= 0.2, as displayed by the upper trace in Fig.3.

When the intracavity etalons are inserted into the laser cavity of the above case, as shown in Fig.1(a), the output laser power with narrow bandwidth is decreased. Since the intracavity etalons affect the output laser power as a loss, we define an effective transmissivity of the set of the two etalons T_e (<1) in the laser cavity. The effective reflectivities for the laser cavity are then given

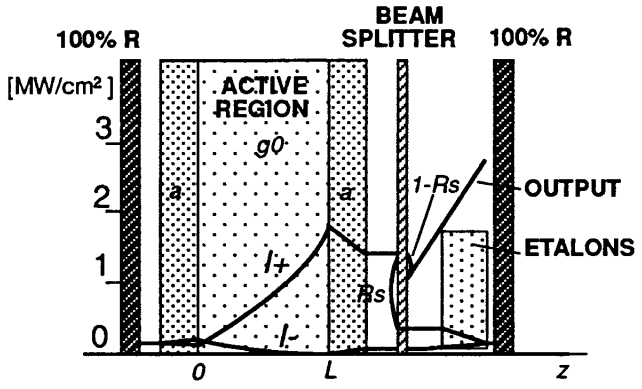

Fig.4 Schematic representation of the laser propagation model for the laser with a beam splitter for power extraction.

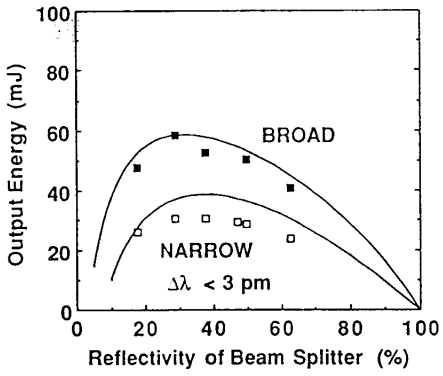

Fig.5 Dependence of the output energy on reflectivity of the output mirror for the laser with a beam splitter. The traces are calculated from eqs.(3), (4), and (5). Upper trace: broad band laser output without intracavity etalons. Lower trace: narrow band laser output with intracavity etalons.

by

$$R_a = (1 - a)^2 T_e^2 \qquad \text{and} \qquad R_b = (1 - a)^2 R \ . \tag{5}$$

Substituting eqs.(5) into eqs.(3), the effective transmissivity T_e is determined so that the calculated results will agree with the experimental data for the laser with intracavity etalons shown in Fig.3. The best fit of the data gave $T_e = 45$ % as displayed by the lower trace in Fig.3.

Using the obtained parameters g_0, I_s, a, and T_e, we estimated the performance of the laser with a beam splitter for power extraction with and without the intracavity etalons. A schematic representation of the laser propagation model for the laser is shown in Fig.4. The effective reflectivities for this cavity are expressed as

$$R_a = (1 - a)^2 \qquad \text{and} \qquad R_b = (1 - a)^2 R_s^2 T_e^2 \ , \tag{6}$$

where R_s is the reflectivity of the beam splitter, and the effective transmissivity T_e is 45% or 100% with or without the etalons, respectively. Figure 5 shows the dependence of the laser output energy on the reflectivity of the beam splitter with and without the intracavity etalons. The calculated traces show good agreements with the experimental data. It should be noted from these results that the laser propagation model is also applicable for estimating the performance of the laser with a beam splitter.

4. DISCUSSION

A comparison of output energies of the conventional and self-injection lasers is given by Figs.3 and 5. For the broad band oscillation without intracavity etalons, the maximum output energy of the laser with a beam splitter (≈ 60 mJ) is somewhat lower than that of the laser with the conventional cavity (≈ 80 mJ) because there is a fraction of the laser beam that escapes through the beam splitter from the spectral-narrowing branch. On the other hand, with narrow bandwidth, the maximum output energy of the laser with a beam splitter is the same (> 30 mJ) as that of the laser with the conventional cavity. It is readily estimated from these results that the power loss at the intracavity etalons in the laser cavity with a beam splitter is much smaller than that in the conventional one.

A portion of the laser power is dissipated at the intracavity etalons in the round trip due to absorption mainly by the dielectric coatings. Since the amount of the dissipated power at the etalons would depend on the laser intensity passing through them, we can estimate the thermal stress of the etalons by calculating the laser intensity incident on them from the discharge chamber. The

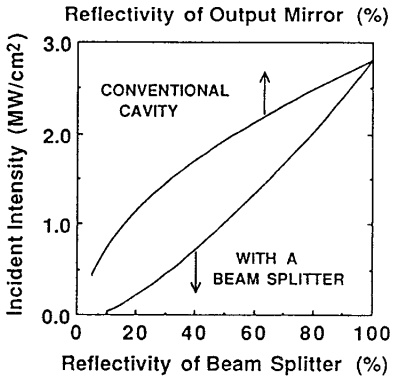

Fig.6 Laser intensity incident on the intracavity etalons vs. reflectivities of either output mirror or beam splitter.

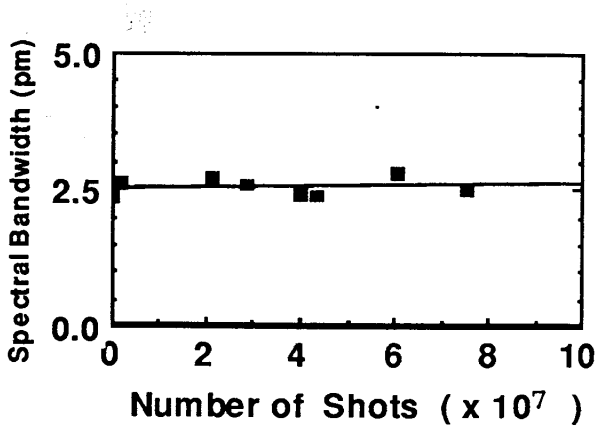

Fig.7 Typical measurements on the spectral bandwidth of the self-injection KrF laser during the total shot of 8 x 10^7. The laser was stabilized to a specific output power of > 2 W at 200 Hz.

calculation was carried out for both configurations of the civities. The results are shown in Fig.6 as a function of the reflectivities of either the beam splitter or the output mirror according to the cavity configurations. In the low-reflection regions in Fig.6, the laser intensity incident on the etalons for the laser with a beam splitter (≈ 0.4 MW/cm^2) is between only 20% and 30% of that for the laser with the conventional cavity (≈ 1.5 MW/cm^2). In these regions, the output energy of the laser with a beam splitter is optimum, as shown in Fig.5. Therefore, by making use of the beam splitter, the laser intensity incident on the etalons can be reduced to less harmful level compared with that in the conventional Fabry-Perot cavity. As a result, the optical damage of the intracavity etalons would be reduced. Additionally, the drift in wavelength due to thermal strain of the etalons at high repetition rate operation can also be minimumized.

An example of the long term spectral purity of the self-injection KrF laser is demonstrated in Fig.7. During 80 million shots, the spectral bandwidth remains approximately constant to within 3 pm FWHM. We expect the spectral bandwidth will remain within 3 pm FWHM beyond several hundred million shots.

5. CONCLUSION

We have reported a new concept for a self-injection KrF excimer laser with narrow bandwidth. In order to reduce the laser intensity incident on the intracavity etalons, a beam splitter was inserted into the laser cavity. The output energies of the laser were in good agreement with the calculated results using the parameters obtained from the laser propagation model for the laser with the conventional laser cavity. The laser intensities incident on the intracavity etalons were calculated for the lasers with a beam splitter and with the conventional Fabry-Perot cavity. It was shown that less laser intensity is incident on the etalons in the cavity with a beam splitter than in the conventional laser cavity. This simple optical arrangement gives an advantage of lower incident intensity on the etalons and provides a reliable spectral performance of spectrally narrowed and high repetition rate excimer lasers.

REFERENCES

1. T. J. McKee, "Spectral-narrowing techniques for excimer laser oscillators," Can. J. Phys. **63**, pp.214-219 ,1985.
2. Y. Shimada, K. Wani and Y. Ogata, "Pressure-controlled wavelength stabilization of a KrF excimer laser with narrowed bandwidth," Jpn. J. Appl. Phys. **28**, pp.2354-2356, 1989.
3. K. Wani, Y. Ogata, Y. Watarai, T. Ono, T. Miyata, R. Sano and Y. Terui, "Narrow-band KrF excimer laser — tunable and wavelength stabilized," Proc. of SPIE, *Excimer Beam Applications*, Vol.988, pp.2-8, SPIE, Boston, 1988.
4. T. H. Dunning, Jr. and P. J. Hay, "The covalent and ionic states of the rare gas monofluorides," J. Chem. Phys. **69**, pp.134-149, 1978.
5. W. W. Rigrod, "Saturation effects in high-gain lasers," J. Appl. Phys. **36**, pp.2487-2490, 1965.
6. J. K. Rice, G. C. Tisone and E. L. Patterson, "Oscillator performance and energy extraction from a KrF excimer laser pumped by a high-intensity relativistic electron beam," IEEE J. Quantum Electron. **QE-16**, pp.1315-1326,1980.